The pion transition form factor and the pion distribution amplitude.

S. Noguera* and V. Vento†

Departamento de Física Teórica and Instituto de Física Corpuscular,
Universidad de Valencia-CSIC, E-46100 Burjassot (Valencia), Spain.
(Dated: January 21, 2014)

Recent BaBaR data on the pion transition form factor, whose Q^2 dependence is much steeper then predicted by asymptotic Quantum Chromodynamics (QCD), have caused a renewed interest in its theoretical description. We present here a formalism based on a model independent low energy description and a high energy description based on QCD, which match at a scale Q_0. The high energy description incorporates a flat pion distribution amplitude, $\phi(x) = 1$, at the matching scale Q_0 and QCD evolution from Q_0 to $Q > Q_0$. The flat pion distribution is connected, through soft pion theorems and chiral symmetry, to the pion valance parton distribution at the same low scale Q_0. The procedure leads to a good description of the data, and incorporating additional twist three effects, to an excellent description of the data.

I. INTRODUCTION

The implications of recent data by the BaBar Collaboration [1] on the transition form factor $\gamma^* \gamma \to \pi^0$, in our understanding of the structure of the pion are being widely discussed [2–6]. These results have cast doubts on our understanding on the behavior, as a function of the light-cone momentum fraction x, of the pion distribution amplitude(πDA) $\phi_\pi(x)$ [7, 8]. Some investigations have produced scenarios where the pion πDA is flat, i.e. a constant value for all x [2, 3], and are in good agreement with the data for the form factor. These scenarios are compatible with QCD sum rules [8] and lattice QCD [9, 10] calculations which provide values for the second moment of the πDA which are large compared with the asymptotic value $6x(1-x)$ [7] [1]. Model calculations, Nambu-Jona-Lasinio (NJL) [11–13] and the "spectral" quark model [15] give a constant pion distribution amplitude, $\phi(x) = 1$. The pion transition form factor calculated in these models, however, overshoots the data [16].

In here we present a formalism to calculate the pion transition form factor (πTFF) which provides an excellent description in the whole range of experimental data. The formalism consists of three ingredients: *i*)a low energy description of the πTFF; *ii*) a high energy description of the πTFF; *iii*) a matching condition between the two descriptions at a scale Q_0 characterizing the separation between the two regimes. For the low energy description we take a parametrization of the low energy data to avoid model dependence at Q_0. The high energy description of the πTFF, defined by the pion Distribution Amplitude (πDA), contains Quantum Chromodynamic (QCD) evolution from Q_0 to any higher Q, the recently introduced mass cut-off procedure [2], and ultimately additional higher twist effects. The relation between the leading twist (πDA) and the pion Parton Distribution (πPD) allows us to use a scheme for the determination of Q_0 that has proven successful to describe parton distributions of mesons and baryons [17–23]. The scheme consists in evolving the second moments of the parton distributions from a scale where they are experimentally known to a scale Q_0 where they coincide with those determined by a low energy description. Once Q_0 is known, higher Q results for any other observable are obtained by evolving the low energy description of the corresponding observable from Q_0 to the required scale Q. Our analysis will systematically explore the region of validity of the scheme and find implications of new physics in the intermediate energy region.

In section II we define the πTFF both for low and high energies and establish the matching condition at the hadronic scale Q_0 . The matching condition of section II allows to determine the mass parameter of the formalism once the hadronic scale is known. Section III is devoted to establish a relation between the πDA and the πPD. This relation allows to characterize a unique matching scale Q_0. Section IV is dedicated to analyze the stability of the parameters and the description of the data. We find reasonable agreement with the experimental data for Q^2 below 15 GeV^2 with parameters whose values are to be expected from physical arguments. Two matching scales are investigated in the analysis. We realize that none of them is able to reproduce accurately the slope of the data in

---

*Electronic address: Santiago.Noguera@uv.es
†Electronic address: Vicente.Vento@uv.es
[1] We normalize our πDA to 1.

the intermediate region. In section V we incorporate in a phenomenological way additional twist three effects. They lead to a modification of the matching condition. Their overall effect is small at high Q but they are important in reproducing the slope in the intermediate region. In this way we are able to get an excellent agreement with the data. In section VI we draw some conclusions. Finally, in the Appendix we present a model calculation which overshoots the data and therefore signals the importance of evolution in the description of the experiment. Morevoer, it also serves to understand the order of magnitude of some of the parameters used in our approach.

II.   THE PION TRANSITION FORM FACTOR.

The form factor $F_{\gamma^*\gamma^*\pi}$ relating two photons (real or virtual) to the pion is a very important object of study in exclusive processes in QCD. In particular it has been used by comparing perturbative QCD predictions with experimental data to obtain information about the shape of the πDA[7, 24, 25]. Experimentally for small virtuality of one of the photons it has been measured by the CELLO [26], by the CLEO [27] and recently by the BaBaR [1] collaboration. The last results are in disagreement with previous theoretical expectations.

In lowest order of perturbative QCD, the transition form factor for the process $\pi^0 \to \gamma\gamma^*$ is given by

$$Q^2 F(Q^2) = \frac{\sqrt{2}f_\pi}{3} \int_0^1 \frac{dx}{x} \phi_\pi(x, Q^2). \tag{1}$$

where $Q^2 = -q^2$, q_μ is the momentum of the virtual photon, $\phi_\pi\left(x, Q^2\right)$ is πDA at the Q^2 scale and $f_\pi = 0.131$ GeV. In this expression, the Q^2 dependence appears through the QCD evolution of the πDA. The πDA can be expressed in terms of the Gegenbauer polynomials [28, 29] ,

$$\phi_\pi(x, Q^2) = x\left(1-x\right) \sum_{n(even)=0}^{\infty} a_n\, C_n^{3/2}(2x-1) \left(\log \frac{Q^2}{\Lambda_{QCD}^2}\right)^{-\gamma_n}, \tag{2}$$

where γ_n are the anomalous dimensions

$$\gamma_n = \frac{C_F}{\beta} \left(1 + 4\sum_{k=2}^{n+1} \frac{1}{k} - \frac{2}{(n+1)(n+2)}\right), \tag{3}$$

$\beta = \frac{11N_C}{3} - \frac{2N_f}{3}$ is the beta function to lowest order and $C_F = \frac{N_C^2-1}{2N_C}$. Assuming that the a_n coefficients are known, Eq. (1) gives the πTFF for any value of Q high enough compared with Λ_{QCD}. The a_n coefficients are obtained if we know the πDA, $\phi_\pi\left(x, Q_0^2\right)$, at some momentum Q_0, using the orthogonality relations of the Gegenbauer polynomials

$$a_n \left(\log \frac{Q_0^2}{\Lambda_{QCD}^2}\right)^{-\gamma_n} = 4\frac{2n+3}{(n+1)\left(n+2\right)} \int_0^1 dx\, C_n^{3/2}(2x-1)\, \phi_\pi\left(x, Q_0^2\right) \tag{4}$$

In order to prevent divergences in the integrand of Eq. (1) it has been assumed that $\phi_\pi\left(x\right)$ vanishes for $x = 0$. There are no fundamental reasons for this restriction, moreover, several chiral models predict for massless pions $\phi_\pi(x) = 1$ [11–14]. We use this model prediction as input at Q_0 in Eq (4) and we obtain for the expansion of the πDA

$$\phi_\pi(x, Q^2) = 4x(1-x) \sum_{n(even)=0}^{\infty} \frac{2n+3}{(n+1)(n+2)} C_n^{3/2}(2x-1) \left(\frac{\log\left(Q^2/\Lambda_{QCD}^2\right)}{\log\left(Q_0^2/\Lambda_{QCD}^2\right)}\right)^{-\gamma_n}. \tag{5}$$

This expression has the right asymptotic behavior, $\lim_{Q\to\infty} \phi_\pi(x, Q) = 6x\left(1-x\right)$. Nevertheless, despite its appearance, the πDA defined in Eq. (5) has the properties $\lim_{x\to 0^+} \phi_\pi(x, Q_0) = \lim_{x\to 1^-} \phi_\pi(x, Q_0) = 1$. In order to cure the divergences in the integrand of Eq. (1) we follow the proposal of Radyushkin in section II.B of ref. [2], and we introduce a cutoff mass M in the above definition of the πTFF, in terms of the πDA,

$$Q^2 F(Q^2) = \frac{\sqrt{2}f_\pi}{3} \int_0^1 \frac{dx}{x + \frac{M^2}{Q^2}} \phi_\pi(x, Q^2). \tag{6}$$

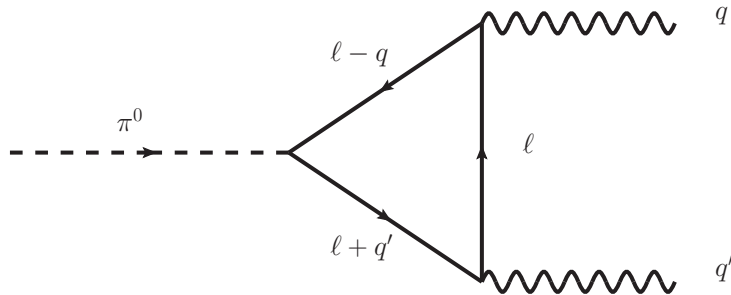FIG. 1: Calculation of the transition form factor via the triangle diagram.

We will discuss later the determination of the M.

At low Q^2 we can parametrize the data as [30],

$$F\left(Q^2\right) = F\left(0\right)\left[1 - a\frac{Q^2}{m_{\pi^0}^2} + ...\right] \tag{7}$$

with $F\left(0\right) = 0.273(10)\,\mathrm{GeV}^{-1}$ and $a = 0.032\,(4)$, constants which have been obtained from the experimental study of $\pi^0 \to \gamma\,e^+\,e^-$. The πTFF at these low values of Q^2 can be described by several hadron models. For instance, the parametrization can be well understood studying the triangle diagram (see Fig. 1). This calculation is straightforward (see appendix) leading, in the case of massless pions, to $F(0) = \sqrt{2}/\left(4\pi^2 f_\pi\right) = 0.273\,\mathrm{GeV}^{-1}$, which coincides with the experimental value. The parameter a can be linked to the constituent quark mass, obtaining $m_q = m_\pi/\sqrt{12\,a} \simeq 0.220\,\mathrm{GeV}$.

Despite the fact that several models reproduce the low energy data, in order to have a model independent expression for the form factor, we adopt a monopole parametrization of the πTFF in the low energy region:

$$F^{LE}\left(Q^2\right) = \frac{F\left(0\right)}{1 + a\frac{Q^2}{m_{\pi^0}^2}}. \tag{8}$$

We have thus introduced two descriptions for the πTFF, one in the low energy regime defined by $F^{LE}(Q^2)$, and one in the high energy regime, defined by Eqs.(5) and (6). Both descriptions will be matched at Q_0, the scale previously introduced which we now define. If $Q > Q_0$ the pion form factor should be calculated using Eqs. (5) and (6), and for $Q < Q_0$ by Eq. (8). For $Q = Q_0$ both expressions should lead to the same result. In this way Q_0 is defined as the matching point between the low and high energy descriptions. Consistency implies that this matching point must be the same for any physical quantity.

Note that our formalism contains two unknowns, Q_0 and M. The scale Q_0 is an important ingredient of our calculation [18–20] and determines the range of validity of the low energy description used in the calculation, i.e. for $Q < Q_0$ $\phi_\pi(x) = 1$ and $F^{LE}\left(Q^2\right)$ is assumed to be a good representation of the theory. Q_0 is fixed by the value of Λ_{QCD}, and the physical results should not show any dependence on it. M contains not only the effects associated with the constituent quark mass but, as pointed out by Radyushkin [2], also the contribution of some mean transverse momentum.

We next equate the pion form factor calculated via equation (6) at $Q^2 = Q_0^2$, where $\phi_\pi(x, Q_0) = 1$,

$$Q_0^2 F(Q_0^2) = \frac{\sqrt{2}f_\pi}{3}\int_0^1 \frac{dx}{x + \frac{M^2}{Q_0^2}} = \frac{\sqrt{2}f_\pi}{3}ln\frac{Q_0^2 + M^2}{M^2}, \tag{9}$$

to the value given by the monopole parametrization Eq. (8),

$$\frac{\sqrt{2}f_\pi}{3}ln\frac{Q_0^2 + M^2}{M^2} = Q_0^2 F^{LE}(Q_0^2) = \frac{F\left(0\right)Q_0^2}{1 + a\frac{Q_0^2}{m_{\pi^0}^2}}. \tag{10}$$

This is the first equation relating the two parameters. We proceed in the next section to find a second relation relation which allows a full determinations of the parameters.

III. THE PION DISTRIBUTION AMPLITUDE AND THE PION PARTON DISTRIBUTION.

In this section we establish a relation between the πDA and the pion valence parton distribution (πVPD) which will be instrumental in the determination of Q_0.

The πDA is defined by,

$$\delta_{ij}\, i\, \sqrt{2}\, f_\pi\, \phi_\pi\,(x) = \int \frac{d\lambda}{2\pi}\, e^{i\lambda x}\, \langle 0|\, \bar\psi\,(0)\, \gamma^+ \gamma_5 \tau^i \psi\,(\lambda n)\, \big|\pi^j\,(P)\big\rangle . \tag{11}$$

In order to introduce a convenient expression for the valence parton distribution let us define the quark distribution

$$H_q^{i,j}\,(x) = \frac{1}{2} \int \frac{d\lambda}{2\pi} e^{i\lambda x}\, \big\langle \pi^i\,(P)\big|\, \bar\psi\,(0)\, \gamma^+ \frac{1}{2}\,\big(1 + \alpha\,\tau^3\big)\, \psi\,(\lambda n)\, \big|\pi^j\,(P)\big\rangle = \frac{1}{2}\,\big(\delta_{i,j}\, H^{I=0}\,(x) + i\epsilon_{i3j}\, \alpha\, H^{I=1}\,(x)\big) \tag{12}$$

with $\alpha = \pm 1$ for $q = u, d$ and $H^{I=0,1}\,(x)$ represent the isospin decompositions. The quark distribution is only non-vanishing in the interval $-1 \le x \le 1$. This quark distribution is related with the standard $q\,(x)$ and $\bar q\,(x)$ distributions, by

$$H_q^\pi = q\,(x)\, \theta\,(x) - \bar q\,(-x)\, \theta\,(-x)\ , \tag{13}$$

with

$$H_u^{\pi^+} = H_d^{\pi^-} = \frac{1}{2}\,\big(H^{I=0}\,(x) + H^{I=1}\,(x)\big)\ . \tag{14}$$

$$H_d^{\pi^+} = H_u^{\pi^-} = \frac{1}{2}\,\big(H^{I=0}\,(x) - H^{I=1}\,(x)\big)\ . \tag{15}$$

The pion valence parton distribution (πVPD) is defined as $H_{Vq}^\pi\,(x) = H_q^\pi\,(x) + H_q^\pi\,(-x)$. Using charge conjugation, one can prove that the isoscalar and isovector part the quark distribution, $H^{I=0,1}\,(x)$, are respectively odd and even functions of x. Therefore

$$H_{Vq}^{i,j}\,(x) = \frac{1}{2} \int \frac{d\lambda}{2\pi} e^{i\lambda x}\, \big\langle \pi^i\,(P)\big|\, \bar\psi\,(0)\, \gamma^+ \frac{1}{2}\, \alpha\,\tau^3 \psi\,(\lambda n)\, \big|\pi^j\,(P)\big\rangle$$
$$+ \frac{1}{2} \int \frac{d\lambda}{2\pi} e^{-i\lambda x}\, \big\langle \pi^i\,(P)\big|\, \bar\psi\,(0)\, \gamma^+ \frac{1}{2}\, \alpha\,\tau^3 \psi\,(\lambda n)\, \big|\pi^j\,(P)\big\rangle \tag{16}$$

In terms of the standard q and $\bar q$ distributions we have

$$H_{Vq}^{i,j}\,(x) = \frac{1}{2}\alpha\, i\, \epsilon_{i3j}\, [q_V\,(x)\, \theta\,(x) + q_V\,(-x)\, \theta\,(-x)] \tag{17}$$

with $q_V\,(x) = q\,(x) - \bar q\,(x)$.

Soft pion theorems have been used to relate the double pion distribution amplitude to the πDA[31]. Using the same arguments, it is easy to connect the matrix elements of the preceeding definitions,

$$\lim_{P\to 0}\, \big\langle \pi^i\,(P)\big|\, \bar\psi_f\,(0)\, \gamma^+ \tau^3 \psi_f\,(\lambda n)\, \big|\pi^j\,(P)\big\rangle = i\, \epsilon_{i3\ell}\, \frac{\sqrt{2}}{i\, f_\pi}\, \lim_{P\to 0}\, \langle 0|\, \bar\psi_f\,(0)\, \gamma^+ \gamma_5 \tau^\ell \psi_f\,(\lambda n)\, \big|\pi^j\,(P)\big\rangle . \tag{18}$$

and therefore

$$H_{Vq}^\pi\,(x) = \frac{1}{2}\,(\alpha)\, i\, \epsilon_{i3j}\, [\phi_\pi\,(x)\, \theta\,(x) + \phi_\pi\,(-x)\, \theta\,(-x)]. \tag{19}$$

Substituiting Eq. (18) in Eq. (16) we obtain

$$\phi_\pi(x) = q_V(x), \tag{20}$$

a relation which is important for our scheme because it provides a universal determination of the hadronic scale Q_0.

The previous result, Eq.(20), is confirmed by chiral models for the pion, like the NJL model or the spectral quark model. In fact, these local chiral quark models give, in the chiral limit, $\phi_\pi(x) = q(x) = 1$. Using the results obtained in the NJL model for the πDA (see [13]) and the πPD (see [33]) we obtain

$$\phi_\pi\,(x) = 1 + \mathcal{O}\,\big(m_\pi^2\big)\ , \qquad q_V\,(x) = \frac{g_{\pi qq}\, f_\pi}{\sqrt{2}\, m_q} + \mathcal{O}\,\big(m_\pi^2\big) = 1 + \mathcal{O}\,\big(m_\pi^2\big) \tag{21}$$

where in the last relation m_q is the constituent quark mass, $g_{\pi qq}$ is the pion quark coupling constant and the last step follows from the Goldberger-Treiman relation. This result for $q_V(x)$ arises naturally from the physical meaning of the πVPD. The flatness of the distribution implies that the probability of finding a quark of any relative momentum fraction x is the same. This is so because in the chiral limit quarks and pions are massless and therefore there is no mass scale to which the momentum distribution can attach. The appearance of flat distributions is a fundamental consequence of soft pion theorems and the chiral limit, not a peculiarity of some models.

Since the origin of the flat distribution is related to soft pion theorems and the chiral limit, this behavior will change as we move towards higher energy. Starting from Q_0, the momentum scale in which the flat distributions are a good approximation, $\phi_\pi(x, Q_0) = q_V(x, Q_0) = 1$, we apply the evolution equations in order to obtain these distributions at higher Q values. The πVPD, $q_V(x, Q)$ evolves through the DGLAP equation, and it concentrates close to the $x \sim 0$ region for very high values of Q. The πDA evolves through the ERBL equation and, therefore, for high Q values we obtain the asymptotic result $\phi_\pi(x, Q) \sim 6x(1-x)$. In conclusion, QCD evolution obscures the relation between these two distributions, which become distinct from one another. It follows from the above discussion that it is unreasonable to assume that at relatively low energies $\phi_\pi(x)$ is close to its asymptotic value, whereas the πVPD is far from it.

The evolution of the flat πVPD, $q(x, Q_0) = 1$, has been previously studied in refs. [17, 21–23] obtaining a very good description of the experimental data. We sketch here the procedure to fix the value of the matching point, Q_0. We know that the momentum fraction of each valence quark at $Q = 2\,\text{GeV}$ is 0.23 [32]. We fit the initial point of the evolution, Q_0, imposing that the evolved πVPD reproduces this momentum fraction at $Q = 2\,\text{GeV}$. Obviously, the resulting Q_0 value will depend on the value of Λ_{QCD}. Varying Λ_{QCD} form $0.174\,\text{GeV}$ to $0.326\,\text{GeV}$ we obtain that Q_0 changes from $0.290\,\text{GeV}$ to $0.470\,\text{GeV}$, in leading order (LO) evolution. A change in Λ_{QCD} implies a change in the initial point Q_0 but, once we have fitted Q_0 through the momentum fraction carried by the quarks at $Q = 2\,\text{GeV}$, the evolved parton distribution is independent of the value of Λ_{QCD} and the quality in the description of the experimental data is preserved.

At this point we must return to Eq. (10) regarding the stability of M. We obtain that M changes only a few MeV when we vary Λ_{QCD} form $0.174\,\text{GeV}$ to $0.326\,\text{GeV}$. The largest incertitude comes from the experimental error in a, obtaining $M = 0.466 \pm 0.006\,\text{GeV}$. We thus obtain a very stable value for M, showing the consistency of the procedure. For the numerical analysis we have chosen $\Lambda_{QCD} = 0.226\,\text{GeV}$, $Q_0 = 0.355\,\text{GeV}$, $a = 0.32$ and $M = 0.466\,\text{GeV}$.

IV. DISCUSSION.

Summarizing the ideas developed previously, a model independent scheme of evaluation for the πTFF at high Q values arises under the following assumptions: i) we consider, on the basis of chiral symmetry and soft pion theorems, that at some point Q_0 the πDA and the πVPD coincide and have flat behavior $\phi_\pi(x, Q_0) = q_V(x, Q_0) = 1$; ii) we fix Q_0 applying QCD evolution to the πVPD from Q_0 to $Q = 2\,\text{GeV}$ and impose that each valence quark carries a fraction of the total momentum of the pion of 0.23; iii) for $Q < Q_0$ we assume the experimental parametrization of $F(Q^2)$ given in (8); and iv) for $Q > Q_0$ the πTFF is given by the Eq. (6), where we fix the M parameter through the continuity condition Eq. (10).

In Figs. 2 and 3 we show the πTFF calculated using the evolved πDA as explained above and compare with the data of refs. [1, 26, 27].

In ref. [21] for the pion, and in refs. [19, 20] for the nucleon, it is shown that including gluons and sea quarks at low energy the preferred starting point for evolution is $Q_0 \simeq 1\,\text{GeV}$. To move Q_0 up to $1\,\text{GeV}$ implies to change the value of M to $0.500\,\text{GeV}$. Dashed curves in Fig. 2 and 3 reproduces the πTFF calculated with these parameters. The experimental incertitude in a produces in this case a larger indetermination in the mass, obtaining $M = 0.500 \pm 0.040\,\text{GeV}$. Nevertheless, this error does not affect to the predictive power, as shown in Fig. 2.

The calculation shows several features which we now discuss. The first effect of this model independent calculation, in comparison with the triangle result, is to cure the asymptotic behavior of the form factor. Model calculations overshoot the experimental data for $Q^2 \sim 10-30\,\text{GeV}^2$ as is clear from ref. [16] and it is confirmed by our calculation of the triangle diagram (see appendix), where we obtain $Q^2 F(Q^2) \sim 0.54\,\text{GeV}$ for $Q^2 \sim 30\,\text{GeV}^2$. Moreover, the form factor in this model calculation shows a behavior proportional to $\left[\log\left(Q^2/m^2\right)\right]^2$ for high Q^2. Now, with the procedure defined here, we recover the right asymptotic result $Q^2 F\left(Q^2\right) \to \sqrt{2} f_\pi$. What is under discussion at present is not this value, but for which value of Q^2 the asymptotic behavior is attained and the behaviour of the πTFF in the intermediate energy region.

In Fig. 3 we observe that the calculation with the mass cut-off introduced in ref. [2] adjusts well to the data up to $Q^2 \sim 15\,\text{GeV}^2$, when we use as matching point at $Q_0 = 0.355$ GeV. However, at that momentum most of the new data bend upward while our calculation remains practically flat (see Fig 2). The slope of the πTFF in the region
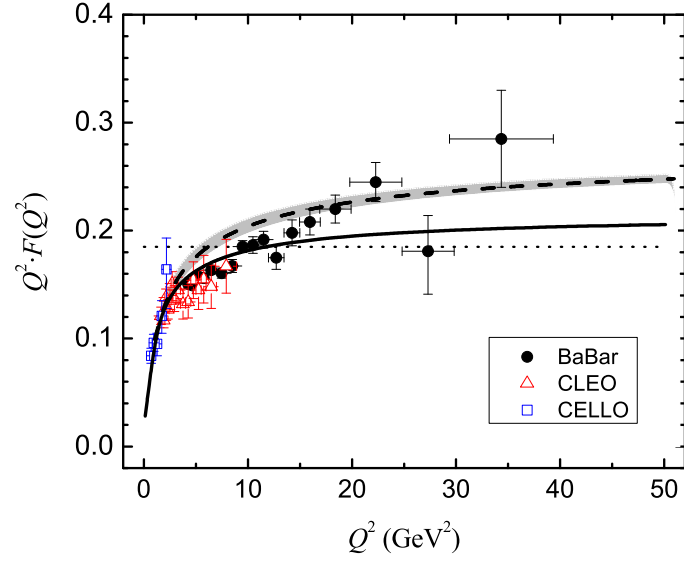
FIG. 2: Calculation of the transition form factor via the πDA with $M = 0.466\,\mathrm{GeV}$, $a = 0.032$ and defining the matching point at $Q_0 = 0.355\,\mathrm{GeV}$ (full-line) compared with the experimental data. The dashed-line corresponds to the same calculation defining the matching point at $Q_0 = 1.\,\mathrm{GeV}$ and with $M = 0.500\,\mathrm{GeV}$. The dotted-line corresponds to the asymptotic limit. The gray region gives the indeterminacy of the results due to the error in a, which is only apreciable for the $Q_0 = 1\,\mathrm{GeV}$ case.
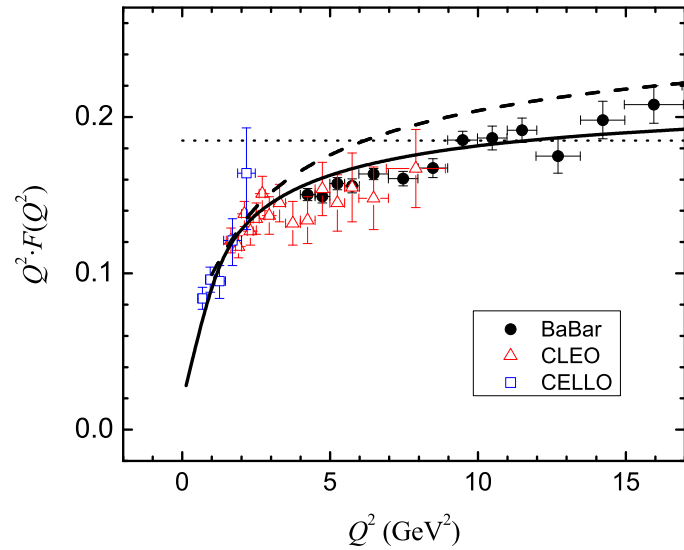
FIG. 3: Same as in Fig 2 for the Q^2 region under $17\,\mathrm{GeV}^2$.

around $20\,\mathrm{GeV}^2$ is not well reproduced. If we assume the higher matching point $Q_0 = 1\,\mathrm{GeV}$, the calculation still fits relatively well the low energy data up to $5\,\mathrm{GeV}^2$, but, contrary to the other, fails in the intermediate region, as we see in Fig. 3. In the region around $20\,\mathrm{GeV}^2$, this calculation goes through most of the experimental points although the slope of the curve is smaller than the one indicated by the data. The indeterminacy in the predictions related to the experimental error in a is only apreciable when we use $Q_0 = 1\,\mathrm{GeV}$ as matching point. It is represented by the gray region in Fig 2, corresponding the upper limit of the region to $a = 0.028$ and the lower limit of to $a = 0.036$. In both calculations, the πTFF tends to the asymptotic limit at very high energy, but in the studied region it is growing very slowly ($Q_0 = 1\,\mathrm{GeV}$ case) or it is practically constant ($Q_0 = 0.355\,\mathrm{GeV}$ case). The value of the mass parameter, around $0.450 - 0.500\,\mathrm{GeV}$, is reasonable, since it receives contributions not only from de constituent quark mass, but also from the mean value of the transverse momentum.

V. POSSIBLE TWIST THREE EFFECTS IN THE PION TRANSITION FORM FACTOR.

Using $Q_0 = 0.355\,\mathrm{GeV}$ as matching point, the experimental results are well reproduced up to $15\,\mathrm{GeV}^2$, but it is difficult to accommodate the higher momentum results. QCD is assymptotically free, and the perturbative approach leading to Eq. (1) must be right for high enough momentum transfer. To correct the high momentum region without touching the low momentum region is not easy, and might require new effects, as the one shown in ref. [6].

On the other hand, using $Q_0 = 1\,\mathrm{GeV}$ as matching point, the high momentum results are well reproduced, but with a too small slope, and the lower momentum data are over estimated. Here we are in a more confortable situation from the point of view of QCD. In order to cure the divergences in the integrand of Eq.(1) we have introduced a cutoff mass M in the definition of the πTFF in terms of the πDA, recall Eq. (6). This procedure incorporates effects of twist three operators at low energy. The set of twist three distribution amplitudes for pions are $\langle 0|\,\bar{d}\,(0)\,i\,\gamma_5\,\tau^i\,u\,(z)\,|\pi^j\rangle$, $\langle 0|\,\bar{d}\,(0)\,\sigma_{\alpha\beta}\,\gamma_5\,\tau^i u\,(z)\,|\pi^j\rangle$ and $\langle 0|\,\bar{d}\,(0)\,\sigma_{\alpha\beta}\,\gamma_5\,\tau^i\,G_{\mu\nu}\,(y)\,u\,(z)\,|\pi^j\rangle$. Some of the effects of these operators are included in the modification proposed by Radyushkin, but there can be additional effects, like the presence of gluons, which are not incorporated in his procedure. These additional effects can be introduced by adding to the lowest order calculation a term proportional to Q^{-2},

$$Q^2 F(Q^2) = \frac{\sqrt{2}f_\pi}{3} \int_0^1 \frac{dx}{x + \frac{M^2}{Q^2}} \phi_\pi(x, Q^2) + \frac{C_3}{Q^2}. \tag{22}$$

The effect of C_3 decreases rapidly with Q^2, and therefore we consider C_3 constant in Q^2. Even though this constant is connected to twist three operators, its QCD evolution is unimportant here.

Following the same ideas developped in Section II, we change the matching condition, Eq (10) in order to introduce the effect of the new term:

$$\frac{\sqrt{2}f_\pi}{3} ln\frac{Q_0^2 + M^2}{M^2} + \frac{C_3}{Q_0^2} = \frac{F\,(0)\,Q_0^2}{1 + a\frac{Q_0^2}{m_{\pi^0}^2}}. \tag{23}$$

With $Q_0 = 1\,\mathrm{GeV}$, this equation allows to determine M, once we have fixed the value of C_3.

We consider three scenarios, which correspond to a contribution from the twist three term to the form factor at $Q_0 = 1\,\mathrm{GeV}$ of 10% ($C_3 = 0.99\,10^{-2}\,\mathrm{GeV}^3$), 20% ($C_3 = 1.98\,10^{-2}\,\mathrm{GeV}^3$) and 30% ($C_3 = 2.98\ 10^{-2}\,\mathrm{GeV}^3$). If we fix[2] $C_3 = 1.98 \cdot 10^{-2}\,\mathrm{GeV}^3$, which implies that this term is responsible for a 20% of the value of the πTFF at $Q_0 = 1\,\mathrm{GeV}$, the experimental error in a produces a variation of $M = 0.620 \pm 0.050\,\mathrm{GeV}$. To check the stability of the M value in relation to C_3, we fix $a = 0.032$ and vary C_3 from $C_3 = 0.99\,10^{-2}\,\mathrm{GeV}^3$ to $C_3 = 2.98\ 10^{-2}\,\mathrm{GeV}^3$. This produces a variation of M given by $M = 0.620 \pm 0.070\,\mathrm{GeV}$. The indeterminacy in M is in all cases of the order of 10%, which is of the same order of the relative error in the experimental determination of a. The value of M is sufficiently stable to confirm the consistency of the procedure. For the numerical analysis we have chosen $\Lambda_{QCD} = 0.226\,\mathrm{GeV}$, $Q_0 = 1.\,\mathrm{GeV}$, $a = 0.032$ and $C_3 = 1.98\,10^{-2}\,\mathrm{GeV}^3$ which corresponds to a 20% contribution of twist 3 at Q_0. This set of parameters implies $M = 0.620\,\mathrm{GeV}$.

---

[2] A dimensionless definition of the parameter C_3 could be $C_3 = a_3\left(m_{\pi^0}^2/a\right)f_\pi$, with a the experimental parameter given in Eq. (8). Therefore, $C_3 = 1.98\,10^{-2}\,\mathrm{GeV}^3$ corresponds to $a_3 = 0.27$. In the Appendix we give the value for C_3 obatined from the triangle diagram.
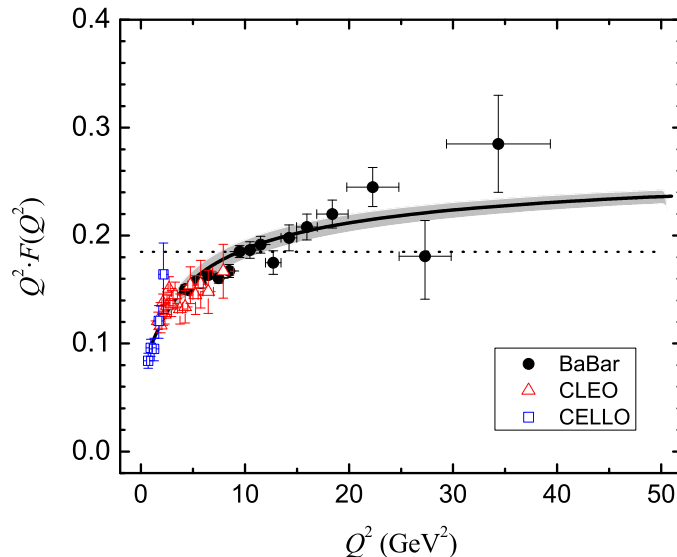
FIG. 4: Calculation of the transition form factor via the πDA with $M = 0.620\,\text{GeV}$, $a = 0.032$, $C_3 = 1.98\,10^{-2}\,\text{GeV}^3$ and defining the matching point at $Q_0 = 1\,\text{GeV}$ (full-line) compared with the experimental data. The gray region gives the indeterminacy of the results due to the indeterminacy on C_3.

In Fig. 4 and 5 we show the πTFF calculated using the evolved πDA compared with the data of [1, 26, 27]. In Fig 5 we have used the experimental parametrization (8) for $Q^2 < 1\,\text{GeV}^2$ (short dashed line). For $Q^2 > 1\,\text{GeV}^2$, the full line corresponds our calculation using Eq. (22) together with the evolved πDA. The gray region corresponds to the effect due to the different contributions of the C_3 term: the upper limit corresponds to $C_3 = 0.99\,10^{-2}\,\text{GeV}^3$ (10% of twist 3 contribution at $Q^2 = 1\,\text{GeV}$); the lower limit corresponds to $C_3 = 2.98\,10^{-2}\,\text{GeV}^3$ (30% of twist 3 contribution at $Q^2 = 1\,\text{GeV}$); the dashed curve in Fig. 5 corresponds to the contribution coming from the C_3 term for our central value, $C = 1.98 \cdot 10^{-2}\,\text{GeV}^3$. We observe that its contribution is absolutely negligible for $Q^2 > 5\,\text{GeV}^2$. Nevertheless, its influence in the matching point is important for a good description of the low Q^2 data. Looking at the whole of the Figs. 4 and 5, we observe that we have a good determination of the experimental data in the whole experimental region.

VI. CONCLUSIONS

In the previous sections we have developed a formalism to describe the πTFF on all experimentally accessible range, and hopefully beyond. The formalism is based on a two energy scale description. The formulation in the low energy scale is non perturbative, while that of the high energy scale is fundamentally a QCD based perturbative formulation. The two descriptions are matched at an energy scale Q_0 hereafter called hadronic scale. This scheme has been applied to described the parton and generalized parton distributions with notable success[18–20, 33]. In order to understand the finesse of the BaBaR data we have forced us to introduce additional ingredients to this scheme which we next summarize.

We have taken for the low energy description of the πTFF a parameterized description of the data. This has been done to avoid model dependence in a region ($Q \sim 1$ GeV), where models might start to break down. The high energy description incorporates the following important physical ingredients: *i)* a mass cut-off in the definition of the πTFF from the πDA, M, [2] which, interpreted from the point of view of constituent models, takes into account the constituent mass, transverse momentum effects and also higher twist effects; *ii)* a flat πDA at low energies in line with chiral models [11–13, 15] and recent proposals [2, 3] ; *iii)* eventually an additional twist three term into the definition of the πTFF in the high energy description parameterized by a unique constant C_3; *iv)* the two descriptions have to match at an energy scale Q_0; this scale is universal and should be the same for all observables. Though our scheme is not based in the use a hadron model, we have presented in the Appendix a simple model calculation to illustrate
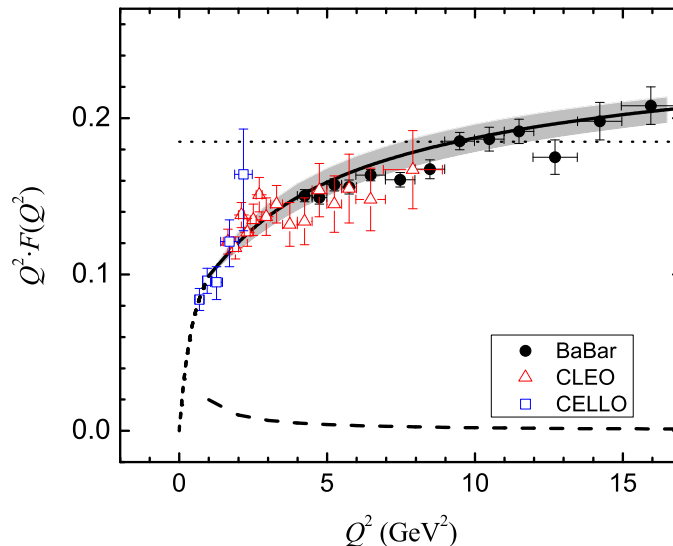
FIG. 5: Same as in Fig 4 for the Q^2 region under $17\,\mathrm{GeV}^2$. The dashed-line corresponds to the C_3 contribution. The short dashed-line is the experimental parametrization (8) for $Q^2 < 1\,\mathrm{GeV}^2$.

the contents of the procedure.

We have seen that, as a consequence of soft pion theorems, the πDA and πVPD are equal at low energies up to the matching scale Q_0. Moreover, chiral models indicate that in the chiral limit both distributions are flat, more precisely, $\phi_\pi(x, Q_0) = q_V(x, Q_0) = 1$. The flatness of the πVPD, which implies that the probability of finding a quark of any relative momentum fraction x is the same, is justified by the fact that in the chiral limit quarks and pions are massless and therefore there is no mass scale to which the momentum distribution can attach. The different tipe of evolution followed by these two distributions hides the relation between them. Nevertheles, the equality between the πDA and the πVPD at Q_0 scale allows us to determine the matching scale using the parton distributions. From previous studies [17, 22, 23] we can fix this scale at $Q_0 = 0.355\,\mathrm{GeV}$. Nevertheless, more elaborated studies [19–21] indicates that this matching scale cannot be one in which the constituent quarks are purely valence but require additional sea and gluon components. Theses studies push the matching scale at $Q_0 \sim 1\mathrm{GeV}$.

Using $Q_0 = 0.355\,\mathrm{GeV}$ as matching point, the experimental results are well reproduce up to $15\,\mathrm{GeV}^2$, but it is difficult to accommodate the higher momentum results. If we adopt this philosophy, the BaBar data, if confirmed, might imply some new type of contributions [6]. Using $Q_0 = 1\,\mathrm{GeV}$ as matching point, the higher momentum results are well reproduced, but with a slope which is too small, and the lower momentum data are overestimated. Nevertheless this last situation can be corrected in a natural way if we assume some additional contribution from twist three.

The calculations shown prove that the BaBar results can be accommodated in our scheme, which only uses standard QCD ingredients and low energy data. It must be emphasized that in order to have a good description higher twist effects are important as the modification from Eq. (1) to Eq. (22) signals. It must be also noted that the matching scale is as high as 1 GeV, a feature which was also the case in the description of parton distributions when precision was to be attained. With these ingredients our calculation shows an excellent agreement with the data and points out that maybe the average value of the highest energy data point is too large, a conclusion reached by other analyses [4, 5].

The relative high value of $M = 0.620\,\mathrm{GeV}$ can be understood on the basis that it includes the constituent quark mass, the mean value of the transverse quark momentum and other higher twist contributions. The C_3 term is relatively small. Its effect is to reduce the value of the contribution to the πTFF of twist two only for low $Q^2 < 5$ GeV^2. Our results are very stable with respect to variations of these parameters.

Let us conclude by stressing that we have developed a formalism to describe the πTFF based on the philosophy that two descriptions, a perturbative and a non perturbative can be matched in a physically acceptable manner at a certain scale Q_0. The idea of the formalism is that one can use models or effective theories to describe the non

perturbative sector while QCD to describe the perturbative one. In here we have preferred to use data for the low energy sector to avoid model dependence, but in other observables, and specially in predictions, models can be used for estimates. Moreover, in order to describe the data we have seen that a matching scale of 1 GeV was favored over the one of 0.355 GeV that we would obtain if only valence constituents were assumed to describe low energies. This implies that the description of high precision data requires sophisticated effective theories (models) at low energies. We have also discovered that higher twist effects (parametrized in our case by M and C_3) are small but crucial in order to attain good descriptions. Finally we can assert that our description of the data is excellent all over although points out to a too large average value of the highest Q points in the data.

Appendix A: The triangle diagram.

The easiest model to evaluate the πTFF is to use the triangle diagram defined in Fig. 1. There are two diagrams, the one depicted an another with the photons exchanged. The amplitude for the process can be defined as

$$\mathcal{T} = 4\pi\,\alpha\,\varepsilon^\mu\,\varepsilon'^\nu\,q^\pi\,q'^\sigma\,\varepsilon_{\mu\nu\rho\sigma}\,F\left(q,q'\right) \tag{A1}$$

In a straightforward calculation[3],

$$F(q^2,q'^2) = 8\,m_q\,g_{\pi qq}\,I(m,q^2,q'^2), \tag{A2}$$

where

$$I(m,q^2,q'^2) = i \int \frac{d^4\ell}{(2\pi)^4} \frac{1}{\left(\ell^2 - m_q^2 + i\epsilon\right)\left[(q-\ell)^2 - m_q^2 + i\epsilon\right]\left[(q'+\ell)^2 - m_q^2 + i\epsilon\right]}\ , \tag{A3}$$

q_μ and q'_μ are the photon momenta, which, in this expression, can be real or virtual photons. Here, m_q is the constituent quark mass, $g_{\pi qq}$ the pion-quark coupling constant, q and q' the photons momenta. The small virtuality of one of the photons implies that $q'^2 = 0$, and we define $F(Q^2) = F(q^2, 0)$ with $Q^2 = -q^2$. In the chiral limit, $m_\pi = 0$, we can use the Goldberger-Treiman relation, $g_{\pi qq}/m_q = \sqrt{2}/f_\pi$, obtaining

$$F(Q^2) = \frac{\sqrt{2}\,m_q^2}{2\,\pi^2\,f_\pi} \int_0^1 dx \frac{1}{Q^2 x\sqrt{1+2\,u}} \log\left|\frac{1+u+\sqrt{1+2\,u}}{1+u-\sqrt{1+2\,u}}\right| \tag{A4}$$

where $u = 2m_q^2/(Q^2 x^2)$.

The behavior of the form factor for small Q^2 values follows from the previous equation,

$$F(Q^2) \xrightarrow[Q^2\to 0]{} \frac{\sqrt{2}}{4\pi^2 f_\pi}\left(1 - \frac{Q^2}{12\,m_q^2}\right) \tag{A5}$$

Therefore, we have $F(0) = \sqrt{2}/\left(4\pi^2 f_\pi\right) = 0.273\,\mathrm{GeV}^{-1}$, and ,from Eq. (7), $m_q = m_\pi/\sqrt{12\,a} \simeq 0.220\,\mathrm{GeV}$.

We can also look for the asymptotic behavior. The denominator of Eq. (A4) can be developed in the form $x\sqrt{1+2\,u} \sim x + 2m_q^2/(Q^2 x)$. Comparing this expression with Eq. (6), we have $M = \sqrt{2m_q^2/x} \sim 2m_q = 0.44\,\mathrm{GeV}$. Performing the integral in Eq. (A4) we have

$$Q^2 F(Q^2) \xrightarrow[Q^2\to\infty]{} \frac{m_q^2}{2\sqrt{2}\,\pi^2\,f_\pi} \log\frac{Q^2}{m_q^2}\left[\log\frac{Q^2}{m_q^2} + 4\,\frac{m_q^2}{Q^2} + ...\right]...\ . \tag{A6}$$

---

[3] A detailed calculation of this process is shown in ref. [35]. We need to replace there e^2 by $N_c\left(e_u^2 - e_d^2\right) = e^2$, since in our case we have quarks in the loop .

Therefore, the model calculation gives a wrong asymptotic behavior. We have $Q^2 F(Q^2) \sim 0.54\,\text{GeV}$ for $Q^2 \sim 30\,\text{GeV}^2$ which is a very large result, and the form factor grows as $\left(\log Q^2/m_q^2\right)^2$ for large Q^2 values. Comparing this expression with Eq. (22), we obtain $C_3 = \sqrt{2} m_q^4 \log\left(Q_0^2/m_q^2\right)/\pi^2 f_\pi \sim 0.78\,10^{-2}\,\text{GeV}^3$, which is consistent with the values for C_3 used in the text.

[1] B. Aubert *et al.* [The BABAR Collaboration], Phys. Rev. D **80** (2009) 052002 [arXiv:0905.4778 [hep-ex]].
[2] A. V. Radyushkin, Phys. Rev. D **80** (2009) 094009 [arXiv:0906.0323 [hep-ph]].
[3] M. V. Polyakov, JETP Lett. **90** (2009) 228 [arXiv:0906.0538 [hep-ph]].
[4] S. V. Mikhailov and N. G. Stefanis, Mod. Phys. Lett. A **24** (2009) 2858 [arXiv:0910.3498 [hep-ph]].
[5] A. E. Dorokhov, arXiv:0909.5111 [hep-ph].
[6] N. I. Kochelev and V. Vento, arXiv:0912.2172 [hep-ph].
[7] A. V. Efremov and A. V. Radyushkin, Phys. Lett. B **94** (1980) 245.
[8] V. L. Chernyak and A. R. Zhitnitsky, Nucl. Phys. B **201** (1982) 492 [Erratum-ibid. B **214** (1983) 547].
[9] L. Del Debbio, Few Body Syst. **36** (2005) 77.
[10] V. M. Braun *et al.*, Phys. Rev. D **74** (2006) 074501 [arXiv:hep-lat/0606012].
[11] M. Praszalowicz and A. Rostworowski, Phys. Rev. D **64** (2001) 074003 [arXiv:hep-ph/0105188].
[12] E. Ruiz Arriola and W. Broniowski, Phys. Rev. D **66** (2002) 094016 [arXiv:hep-ph/0207266].
[13] A. Courtoy and S. Noguera, Phys. Rev. D **76** (2007) 094026 [arXiv:0707.3366 [hep-ph]].
[14] A. Courtoy, Ph. D. Thesis, Valenia University, 2009.
[15] E. Ruiz Arriola and W. Broniowski, Phys. Rev. D **67** (2003) 074021 [arXiv:hep-ph/0301202].
[16] W. Broniowski and E. R. Arriola, arXiv:0910.0869 [Unknown].
[17] R. M. Davidson and E. Ruiz Arriola, Phys. Lett. B **348** (1995) 163. Acta Phys. Polon. B **33** (2002) 1791 [arXiv:hep-ph/0110291].
[18] M. Traini, A. Mair, A. Zambarda and V. Vento, Nucl. Phys. A **614** (1997) 472.
[19] S. Scopetta, V. Vento and M. Traini, Phys. Lett. B **421** (1998) 64 [arXiv:hep-ph/9708262].
[20] S. Scopetta, V. Vento and M. Traini, Nucl. Phys. A **666** (2000) 14 [arXiv:hep-ph/9907440].
[21] S. Noguera and V. Vento, Eur. Phys. J. A **28** (2006) 227 [arXiv:hep-ph/0505102].
[22] W. Broniowski, E. R. Arriola and K. Golec-Biernat, Phys. Rev. D **77** (2008) 034023 [arXiv:0712.1012 [hep-ph]].
[23] A. Courtoy and S. Noguera, Phys. Lett. B **675** (2009) 38 [arXiv:0811.0550 [hep-ph]].
[24] G. P. Lepage and S. J. Brodsky, Phys. Rev. D **22** (1980) 2157.
[25] V. L. Chernyak and A. R. Zhitnitsky, Phys. Rept. **112** (1984) 173.
[26] H. J. Behrend *et al.* [CELLO Collaboration], Z. Phys. C **49** (1991) 401.
[27] J. Gronberg *et al.* [CLEO Collaboration], Phys. Rev. D **57** (1998) 33 [arXiv:hep-ex/9707031].
[28] G. P. Lepage and S. J. Brodsky, Phys. Lett. B **87** (1979) 359.
[29] D. Mueller, Phys. Rev. D **51** (1995) 3855 [arXiv:hep-ph/9411338].
[30] C. Amsler *et al.* [Particle Data Group], Phys. Lett. B **667** (2008) 1.
[31] M. V. Polyakov, Nucl. Phys. B **555** (1999) 231 [arXiv:hep-ph/9809483].
[32] P. J. Sutton, A. D. Martin, R. G. Roberts and W. J. Stirling, Phys. Rev. D **45** (1992) 2349.
[33] L. Theussl, S. Noguera and V. Vento, Eur. Phys. J. A **20** (2004) 483 [arXiv:nucl-th/0211036].
[34] D. Binosi and L. Theussl, Comput. Phys. Commun. **161** (2004) 76 [arXiv:hep-ph/0309015].
[35] C. Itzykson and J. B. Zuber, *New York, Usa: Mcgraw-hill (1980) 705 P.(International Series In Pure and Applied Physics)*